A&A 440, 647–651 (2005)
DOI: 10.1051/0004-6361:20052866

Astronomy & Astrophysics

New grids of stellar models including tidal-evolution constants up to carbon burning

II. From 0.8 to 125 $M_{\odot}$: the Small Magellanic Cloud ($Z = 0.002-0.004$)⋆

A. Claret

Instituto de Astrofísica de Andalucía, CSIC, Apartado 3004, 18080 Granada, Spain
e-mail: claret@iaa.es

Received 11 February 2005 / Accepted 8 May 2005

Abstract. New stellar models spefically designed for the Small Magellanic Cloud are presented in this paper. In order to take into account the uncertainties in the metal content we computed two grids with different metallicities: $Z = 0.002$ and $Z = 0.004$. The covered mass range is from 0.8 up to 125 $M_{\odot}$ and the models are followed until the exhaustion of carbon in the core, for the more massive ones. We have introduced a recent measurement of the nuclear rate $^{14}N(p,\gamma)^{15}O$. A comparison among models with the old and new rate was carried out revealed that the former are slightly hotter than the first ones. Such differences depend on the mass range. The opacities, the equation of state, the remaining nuclear reactions rates, the core overshooting parameterization and the convective transport of energy are the same as discussed previously by us.
We also give, besides the classical evolutionary models outputs, the internal structure constants needed to investigate apsidal motion and tidal evolution in close binaries. This aspect acquires importance in the light of recent investigations on circularization and synchronization levels in binary systems belonging to the Magellanic Clouds. The role of rotation can also be investigated through the gravity-darkening exponents which allow us to compute the brightness distribution of a given stellar surface.

Key words. stars: abundances – stars: interiors – stars: binaries: eclipsing – stars: rotation

1. Introduction

The investigation of the properties of double-lined eclipsing binaries (DLEB) in the Magellanic Clouds has changed drastically during the last years. Not only are light curves for these objects now available but also better spectroscopic observations. This means that such extragalactic DLEB can be used to test the predictions of theoretical stellar models in different chemical environments. However, the investigations are not only restricted to the absolute dimensions: North & Zahn (2003) analysed the levels of circularization of detached binaries in the SMC and LMC using data from OGLE and MACHO. Still concerning tidal evolution, Faccioli et al. (2005) used about 4695 eclipsing binaries in the LMC, discovered by the MACHO project, to infer their levels of circularization. Moreover, the precise individual distance of DLEB placed in the SMC serve as a fundamental distance indicator that may have important cosmological implications (e.g. Fitzpatrick et al. 2003).

The present grids of models are a continuation of the previous ones (Claret 2004, hereafter Paper I)) and are adequate for the Small Magellanic Cloud. They were computed for two metallicities ($Z = 0.002-0.004$) in order to take into account the observational uncertainties in the metal content (Ribas 2004). In addition to the standard outputs (age, luminosity, log g, effective temperature, etc.) we also make available the parameters needed to follow the tidal evolution of close binaries, such as the depth of the convective envelope $x_{\rm bf}$, the radius of gyration β as well as the tidal torque constant E_2 for stars with higher effective temperatures. The apsidal-motion rates can be also investigated through the harmonics k_2, k_3 and k_4.

We also introduce the calculation of the gravity-darkening exponent β_1 which is necessary to understand how the flux is distributed over the surface of rapid rotating or tidally distorted stars. We have used the method developed by Claret (1998, 2000), based on the triangle strategy of Kippenhahn, to derive β_1 as a function of mass, age, chemical composition, and effective temperature: such calculations superseded the traditional values of 1 and 0.32 for radiative and convective envelopes, respectively.

⋆ Tables 1–60 are only available in electronic form at the CDS via anonymous ftp to cdsarc.u-strasbg.fr (130.79.128.5) or via http://cdsweb.u-strasbg.fr/cgi-bin/qcat?J/A+A/440/647

On the other hand, new advances in the input physics must be implemented in the codes of stellar evolution in order to be able to compare with the mentioned observational data. For example, the recent measurement of the rate for the reaction $^{14}N(p,\gamma)^{15}O$ (Runkle 2003; Formicola et al. 2004) shows the need to update the evolutionary codes. In this paper, we incorporate this new measurement and compare stellar models computed with the old rate (Schröder et al. 1987) with those obtained with the recent one.

Thus, the recent and varied observations carried out in the Small Magellanic Cloud demand a constant updating of stellar evolution codes in order to make available more realistic theoretical material to be compared with the observational data. The present grids of models help explore some aspects of the evolution of the Small Magellanic Cloud.

2. Brief comments on the input physics of the code: the improved rate $^{14}N(p,\gamma)^{15}O$

The basic physical ingredients of the evolution code such as opacities, equation of state, nucleosynthesis, etc were discussed in Paper I. However, for completeness, some details of the input physics used here are given below. The determination of the metal content of the SMC is not a simple task. In order to take into account the observational uncertainties we adopted two values as representative for the SMC ($(X,Z) = (0.754, 0.002)$ and (0.748, 0.004)). Core overshooting was considered taking $d_{ov} = \alpha_{ov} H_p$, where H_p is the pressure scale height and $\alpha_{ov} = 0.20$. The convection was modeled using the standard mixing-length theory with $\alpha = 1.68$. The radiative opacities were adopted from Iglesias & Rogers (1996) for higher temperatures while the results by Alexander & Ferguson (1994) results were adopted for lower temperatures. The screening factors are taken from Graboske et al. (1973) and the loss of energy due to neutrinos was considered using the work by Itoh et al. (1989). The mass loss rates were taken from Nieuwenhuijzen & de Jager (1990) for all models except in two situations: Wolf-Rayet stars and red giants with masses smaller than 4 $M_\odot$. The adopted criterion to consider a star as becoming a Wolf-Rayet is: WNL (hydrogen surface abundance smaller than 0.4 and $T_{\rm eff} \approx 10\,000$ K); WNE (hydrogen-free and no evidence of the products of He-Burning) and WC (evidence of the presence of such products). The parametrization by Langer (1989) was adopted for WNE and WC Wolf-Rayet stars. For the WNL Wolf-Rayet stars, we adopted the formalism by Conti (1988). In such parametrizations, there is no dependence on the metallicity. However, more recent determination of the mass loss rate for Wolf-Rayet stars indeed indicate a dependence not only on metallicity but also on the luminosity (Nugis & Lamers 2000). The adopted rates seem to overestimate the mass loss by a factor of around 0.4 dex. For the red giants, we used the work by Reimers (1977).

In addition to the new rate for $^{14}N(p,\gamma)^{15}O$, we have implemented a more extensive nuclear network with up to 47 isotopes. However, as this version is very CPU consuming, we adopted here a simpler version with 13 isotopes: ^{1}H, ^{4}He, ^{12}C, ^{13}C, ^{14}N, ^{16}O, ^{17}O, ^{18}O, ^{20}Ne, ^{22}Ne, ^{24}Mg, ^{25}Mg and ^{26}Mg.

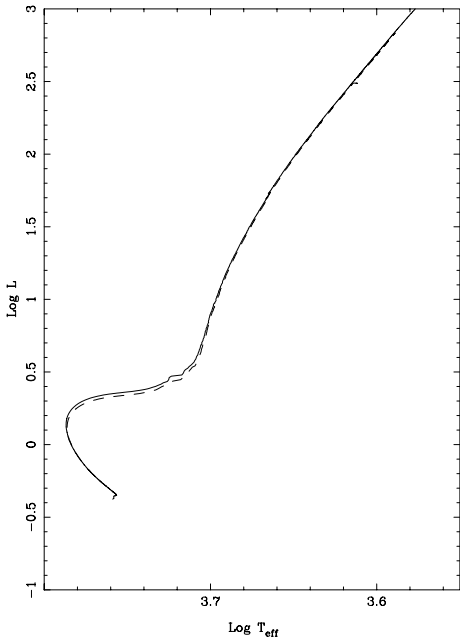

Fig. 1. Comparative HR diagram for a 0.8 $M_\odot$ model. Continuous line represents the track computed using the new $^{14}N(p,\gamma)^{15}O$ rate while dashed one denotes the evolutionary sequence adopting the NACRE rate.

Specifically, for the helium burning we used:
$^{4}He(\alpha,\gamma)^{8}Be(\alpha,\gamma)^{12}C(\alpha,\gamma)^{16}O(\alpha,\gamma)^{20}$ Ne
$^{17}O(\alpha, n)^{20}Ne$
$^{20}Ne(\alpha,\gamma)^{24}Mg$
$^{13}C(\alpha, n)^{16}O$
$^{22}Ne(\alpha, n)^{25}Mg$
$^{22}Ne(\alpha\gamma)^{26}Mg$
$^{14}N((\alpha,\gamma)^{18}F(\beta\nu)^{18}O(\alpha,\gamma)^{22}Ne$
and for carbon burning:
$^{12}C(^{12}C, \alpha)^{20}Ne$
$^{12}C(^{12}C, p)^{23}Na$
$^{23}Na(p, \alpha)^{20}Ne$
$^{12}C(\alpha,\gamma)^{16}O$
$^{16}O(\alpha,\gamma)^{20}Ne$
$^{20}Ne(\alpha,\gamma)^{24}Mg$.

With the exception of $^{14}N(p,\gamma)^{15}O$, all reaction rates were taken from NACRE. We have implemeted this new rate (Runkle 2003; Formicola et al. 2004). As known, this reaction acts as a bottleneck to CNO burning since it is the slowest step of the cycle and the effects on the evolutionary lives of the stars will depend on the stellar masses. The revised rate is around a factor of two smaller than the previous one (Schröder et al. 1987; see also Caughlan & Fowler 1988; and Angulo et al. 1999, NACRE). As the CNO cycle dominates hydrogen burning for stars larger than the Sun, the effects of the new result are expected to be larger for more massive stars.

To investigate the impact of the new rate on the morphology and on the physical properties of the tracks, we selected two models with 0.8 and 10 solar masses. We expect that for a slower rate of $^{14}N(p,\gamma)^{15}O$ the corresponding turnoff points will be brighter. Let us examine in an HR diagram how different the tracks are with the new and old rates. Figure 1 shows

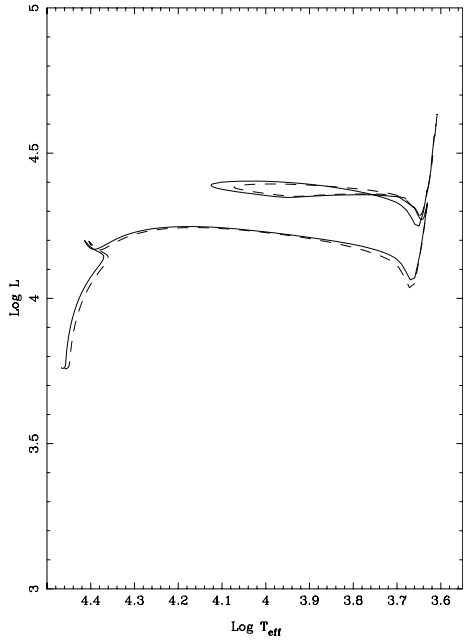

Fig. 2. Comparative HR diagram for a 10 $M_{\odot}$ model. Same remarks as in Fig. 1.

a comparative diagram for a 0.8 $M_{\odot}$ and $Z = 0.002$. The continuous line represents the model computed by adopting the new rate while the dashed one denotes a model based on the old measurement. The tracks are practically indistinguishable up to $\log L \approx 0.2$. However, after the turnoff point the models computed with the improved rate are hotter and brighter, as expected. Of course, this will affect the ages of globular clusters by around 10% (Runkle 2003; Imbriani et al. 2003). The new rate may have cosmological implications too but this is beyond the scope of the present paper. See Imbriani et al. (2004). In Fig. 2 we illustrate the effects of the new rate on a more massive model, 10 $M_{\odot}$. In contrast with the 0.8 $M_{\odot}$, the differences appear at the begining of the hydrogen burning and they are more conspicuous than in the previous case. As can be seen from the figure, the new rate also influences the morphology of the blue loops.

The covered mass range is from 0.8 up to 125 $M_{\odot}$. The models with masses smaller than 1.8 $M_{\odot}$ were followed up to the He-flash; intermediate masses (between 1.99 and 5.01) were followed up to the early asymptotic giant branch and more massive stars were followed up to the exhaustion of carbon in the core. The corresponding HR diagrams for the two grids of models $(X, Z) = (0, 754, 0.002)$ and $(0.748, 0.004)$ are shown in Figs. 3 and 4. For Wolf-Rayet stars, the effective temperatures displayed in such figures correspond to those of the optically thick envelopes. The influence of the metallicity can be noted in the morphology and extension of the blue loops. Figure 5 is particularly interesting for these effects. The actual precision of the determination of effective temperatures seems to be enough to differentiate between both grids. However, as commented in Paper I, there are not many DLEB with more massive stars than about 30 $M_{\odot}$ with good determination of absolute dimensions in order to test the present models with confidence. The situation begun to change with the efforts of E. Guinan and

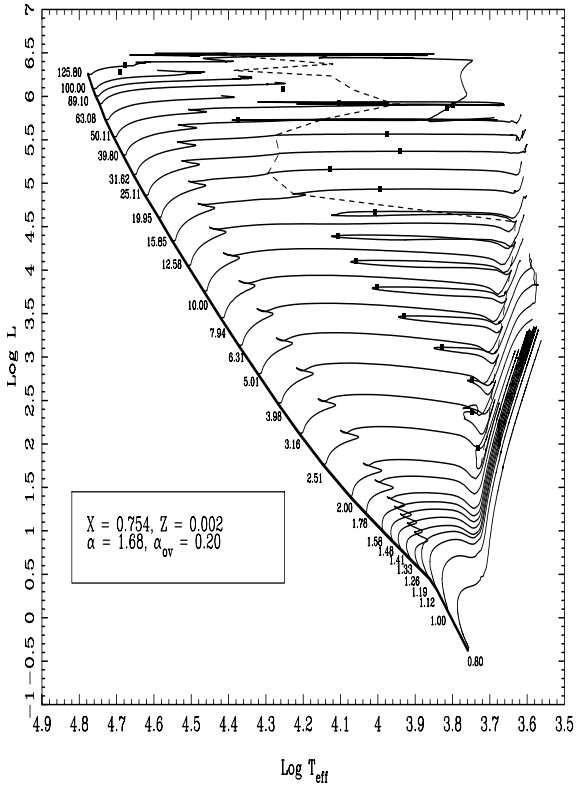

Fig. 3. The theoretical HR diagram for $Z = 0.002$. The numbers below the tracks indicate the stellar masses in solar units. The dashed line indicate the points for which $Y_c = 0.95$ and full squares denote the points for which $Y_c = 0.10$. For the sake of clarity, only Main-Sequence models are shown for $100 < m < 50$ $M_{\odot}$.

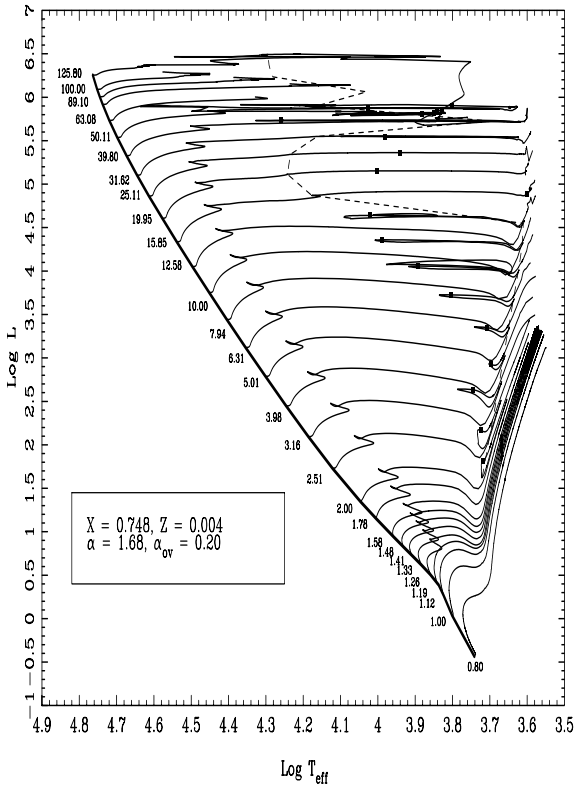

Fig. 4. The theoretical HR diagram for $Z = 0.004$. Same remarks as in Fig. 3.

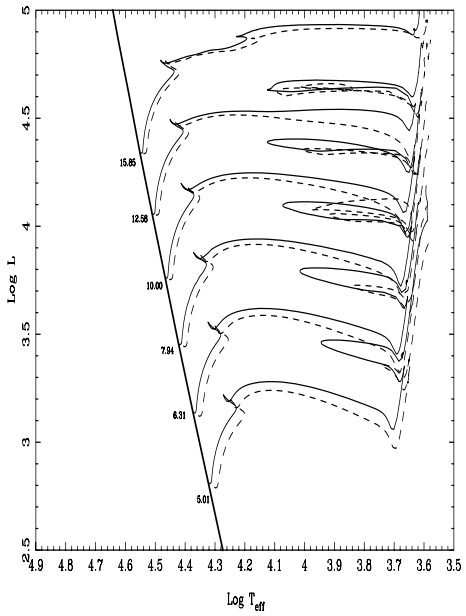

Fig. 5. Differential HR diagram for the grids $(X, Z) = (0.754, 0.002)$ – solid lines – and (0.748, 0.004) – dashed lines.

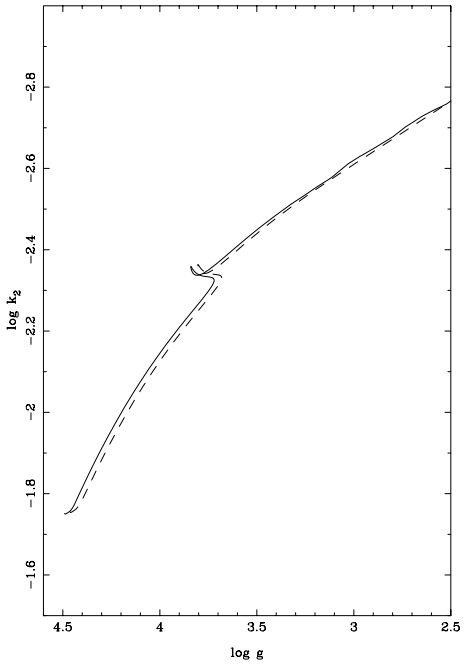

Fig. 6. The apsidal motion constant for a 10 $M_{\odot}$ model as a function of the surficial gravity. Same remarks as in Fig. 1.

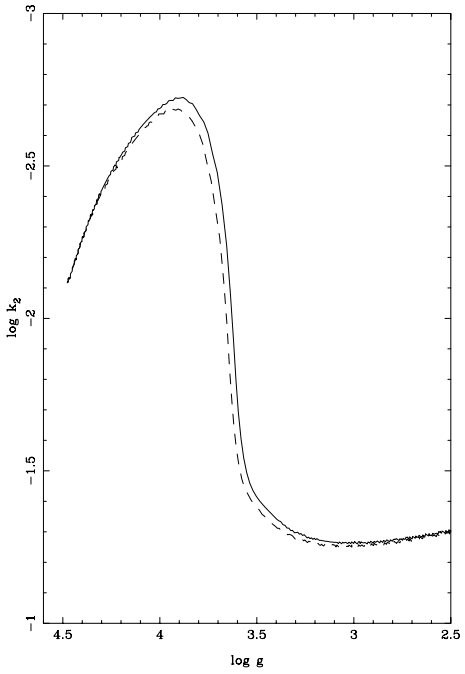

Fig. 7. The apsidal motion constant for a 1.12 $M_{\odot}$ model as a function of the surficial gravity. Same remarks as in Fig. 1.

collaborators (for example, Fitzpatrick et al. 2003) and these new observational data may serve as a good discriminant between the stellar models.

3. Internal structure constants and tidal evolution

The internal structure constants, namely, k_2, k_3 and k_4, which are essential to compute the theoretical apsidal-motion rates in close binaries, are derived by integrating the Radau equation. They are an important test for evolutionary models and also for the predictions of the theory of General Relativity. The calculations presented here are derived within the framework of static tides. In the case of dynamic tides, a more refined treatment is required (see for example Claret & Willems 2002; and Willems & Claret 2003).

The internal structure constants are also affected by the new nuclear rate. Figure 6 shows the behaviour of $\log k_2$ as a function of the surface gravity for the same models of Fig. 2. The new models are slightly more mass concentrated, mainly during the main-sequence. A similar situation can be found for less massive models (Fig. 7) although the differences only appear for more evolved configurations. This is a direct consequence of the internal readjustment of the model under the new physical conditions. The typical deviations are of the order of 0.005 dex.

On the other hand, the investigation of tidal evolution of close binaries in clusters also suffers from the impact of the new observations. For example, the sample of binaries belonging to clusters has increased (Mathieu et al. 2004). Besides this progress, more elaborate theoretical – and auxiliary – concepts of tidal circularization of binaries belonging to clusters were also pointed out: the traditional definition of the cut-off was recently questioned (Meibom 2005; Claret 2005) and this can open new possibilities. The levels of circularization of binaries located in the Magellanic Clouds have been studied in some detail (North & Zahn 2003; Faccioli et al. 2005) and the present grids will be useful in this scenario. As in Paper I, we make available the parameters necessary to integrate the differential equations of tidal evolution: the radius of gyration β, the depth of the convective envelope $x_{\rm bf}$, E (describes a polytropic envelope), the tidal torque constant E_2, etc. Special care was taken to derive $x_{\rm bf}$ to avoid numerical oscillations due to the size of the triangle in the HR diagram. We typically used $\Delta \log T_{\rm eff} = 0.001$ and $\Delta \log L = 0.004$. More details on the

calculations of the tidal-evolution constants and the corresponding differential equations can be found in Paper I.

4. Stellar distortions: rotation and tides

The impact of recent observations of stellar rotation during the last years has been large. Souza et al. (2003) used the VLTI to estimate the stellar shape of Achernar, a B3V type star, and reported that its oblatness is around 1.56 ± 0.05. van Belle et al. (2001) used the Palomar Testbed Interferometer to infer the oblatness of Altair (A7 IV-V) in 1.14 ± 0.03. Another observation of stellar shape comes from a microlens. The gravitational microlensing event MOA2002-BLG-33 was first investigated by assuming that the lensed star, a solar-type one, was spherical (Abe et al. 2003). A more general analysis of the system allowed the same authors to estimate the oblatness of the source star of MOA2002-BLG-33 as 1.02 ± 0.03 (Rattenbury et al. 2005), a value consistent with a slow rotator.

Until very recently, the only source of the effects of stellar distortion came from the close binaries. The shape of the light curves revealed the distortions caused by rotation and tides. The direct measurements of stellar shapes mentioned in the previous paragraph provides an excellent tool to test the theoretical predictions of brightness surface distribution. As is known, the flux depends on the local gravity (von Zeipel 1924). This dependence is characterized by the gravity-darkening exponent β_1, i.e., $F \propto g^{\beta_1}$. Traditionally, β_1 was assumed to be 1.0 (von Zeipel 1924) for stars with radiative envelopes or 0.32 for stars presenting convective outer layers (Lucy 1967). These values are not always valid. A more elaborate numerical method (Claret 1998, 2000) indicated that there is a dependence of β_1 on the dominant mechanism of energy transfer and the evolutionary status of the stellar model. Moreover, a smoother transition for the variation of β_1 between a radiative and convective envelope was found. These theoretical predictions were the subject of a comparison with the β_1 inferred from the analysis of light curves of close binaries provided by Raffert & Twigg (1980). For details of the comparison, see Claret (2003). Additional tests of these β_1 were carried out by Niarchos (2000) and Djurasevic et al. (2003).

As in Paper I, the first five columns of the tables contain the age (in years), $\log L$ (in solar units), $\log g$, $\log T_{\rm eff}$ and the mass (in solar units). Columns 6–9 contain the logarithm of the mass-loss rate ($M_\odot$/year), the logarithm of the central temperature, of the density and the core $q_{\rm c}$ in fraction of the total mass of the star. Columns 10–35 contain the central and surface chemical composition of X, Y, ^{12}C, ^{13}C, ^{14}N, ^{16}O, ^{17}O, ^{18}O, ^{20}Ne, ^{22}Ne, ^{24}Mg, ^{25}Mg and ^{26}Mg. In the next three columns we have $\log k_2$, $\log k_3$ and $\log k_4$. The depth of the convective envelope $x_{\rm bf}$ is given in Col. 39, while $\log E_2$ is given in Col. 40. The constant E, the form factor $\alpha_{\rm P}$ and β are given in positions 41, 42 and 43, and Col. 44 gives the gravity-darkening exponent β_1 (see Paper I for details of the respective equations). The corresponding isochrones will be published elsewhere.

Acknowledgements. I am grateful to V. Costa, who helped to improve the paper. G. Meynet is also acknowledged for helpful comments. The Spanish MCYT (AYA2003-04651) is gratefully acknowledged for its support during the development of this work.

References

Abe, F., Bennett, D. P., Bond, I. A., et al. 2003, A&A, 411, L493
Alexander, D. R., & Ferguson, J. W. 1994, ApJ, 437, 879
Angulo, C., Arnould, M., Rayet, M., et al. 1999, Nucl. Phys. A, 656, 3
Caughlan, G. R., & Fowler, W. A. 1988, ADNDT, 40, 283
Claret, A. 1998, A&AS, 131, 395
Claret, A. 2000, A&A, 259, 289
Claret, A. 2003, A&A, 406, 623
Claret, A. 2004, A&A, 424, 919 (Paper I)
Claret, A. 2005, in Tidal evolution and oscillations in binary stars, ASP Ser., ed. A. Claret, A. Giménez, & J.-P. Zahn, 333, 122
Claret, A., & Willems, B. 2002, A&A, 388, 518
Conti, P. S. 1988, NASA SP-497, ed. P. S. Conti, & A. B. Underhill
Djurasevic, G., Rovithis-Livaniou, H., Rovithis, P., et al. 2003, A&A, 402, 667
Faccioli, L., Alcock, C., Cook, K., Prochter, G., & Syphers, D. 2005, in Tidal evolution and oscillations in binary stars, ASP Ser., ed. A. Claret, A. Giménez, & J.-P. Zahn, 333, 75
Formicola, A., et al. 2004, Phys. Lett. B, 591, 61
Fitzpatrick, E. L., Ribas, I., Guinan, E. F., Maloney, F. P., & Claret, A. 2003, ApJ, 587, 685
Graboske, H. C., De Witt, H. E., Gorssman, A. S., & Cooper, M. S. 1973, ApJ, 181, 457
Imbriani, G., Costantini, H., Formicola, A., et al. 2004, A&A, 420, 625
Iglesias, C. A., & Rogers, F. J. 1996, ApJ, 464, 943
Itoh, N., Adachi, T., Nakagawa, M., Kohyama, Y., & Munakata, H. 1989, ApJ, 339, 354
Langer, N. 1989, A&A, 220, 135
Lucy, L. B. 1967, Z. Astrophys., 65, 89
Mathieu, R.D., Meibom, S., & Dolan, C. J. 2004, ApJ, 602, 621
Meibom, S. 2005, in Tidal evolution and oscillations in binary stars, ASP Ser., ed. A. Claret, A. Giménez, & J.-P. Zahn, 333, 64
Niarchos, P. G. 2000, in Variable Stars as Essential Astrophysical Tools, ed. C. Ibanoglu, 631
Nugis, T., & Lamers, H. J. G. L. M. 2000, A&A, 360, 227
Nieuwenhuijzen, H., & de Jagger, C. 1990, A&A, 231, 134
North, P., & Zahn, J. P. 2003, A&A, 405, 677
Rafert, J. B., & Twigg, L. W. 1980, MNRAS, 193, 79
Rattenbury, N. J., et al. 2005, A&A, in press
Reimers, D. 1977, A&A, 61, 217
Ribas, I. 2004, private communication
Runkle, R. C. 2003, Ph.D. Thesis, University of North Carollina, unpublished
Schröder, U., et al. 1987, Nucl. Phys. A, 467, 240
Souza, D., Kervella, P., Jankov, S., et al. 2003, A&A, 407, L47
van Belle, G. T., Ciardi, D. R., Thompson, R. R., et al. 2001, ApJ, 559, 1155
von Zeipel, H. 1924, MNRAS, 84, 665
Zahn, J. P. 1975, A&A, 41, 329
Zahn, J. P. 1989, A&A, 220, 112
Willems, B., & Claret, A. 2003, A&A, 410, 289